

**EUROPEAN
MECHANICS
SOCIETY**

EUROMECH COLLOQUIUM 513

Dynamics of non-spherical particles in fluid turbulence

06. – 08. April, 2011

Udine, Italy

Lattice Boltzmann simulations for characterizing the behavior of agglomerates with different morphologies

Mathias Dietzel, Prof. Dr.-Ing. Martin Sommerfeld

Mechanische Verfahrenstechnik

Zentrum für Ingenieurwissenschaften

Martin-Luther-Universität Halle-Wittenberg

D-06099 Halle (Saale)



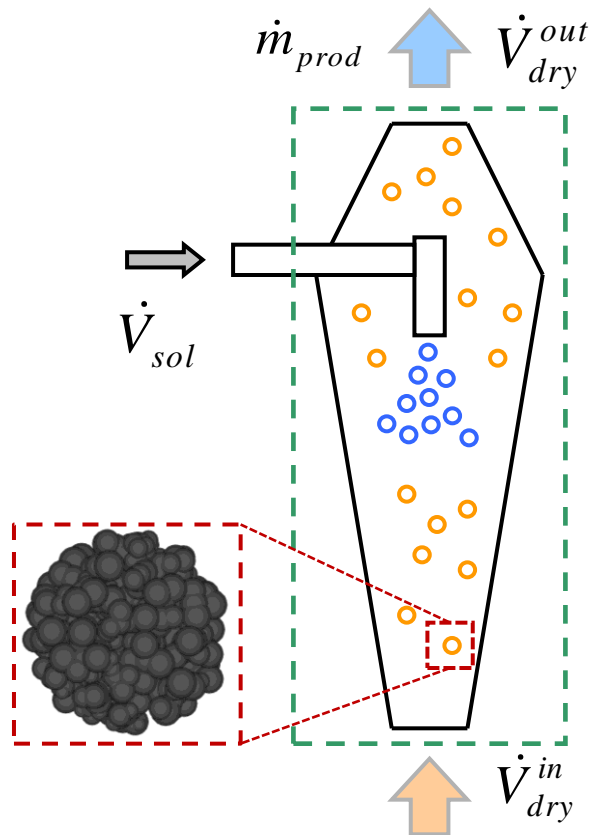
Martin-Luther-Universität
Halle-Wittenberg



Introduction

Motivation

- Investigation of the flow behavior of porous particles:
 - porous particles are relevant in many technical applications (e.g. spray drying, pharmaceuticals, colloidal process engineering)



- multi-scale approach regarding CFD methods: combining DNS and Euler/Lagrange
- level of abstraction depending on numerical approach, available models and computational resources

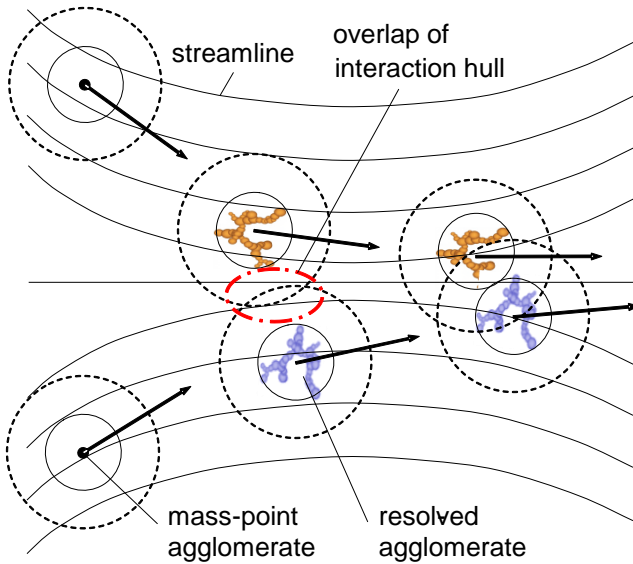
▪ **Euler/Lagrange** simulation on apparatus scale: quantitative prediction of process parameters, low resolution, point-mass model

▪ **Lattice-Boltzmann** simulation on particle scale: modeling elementary processes of transport, mass and heat transfer at high resolution (DNS)

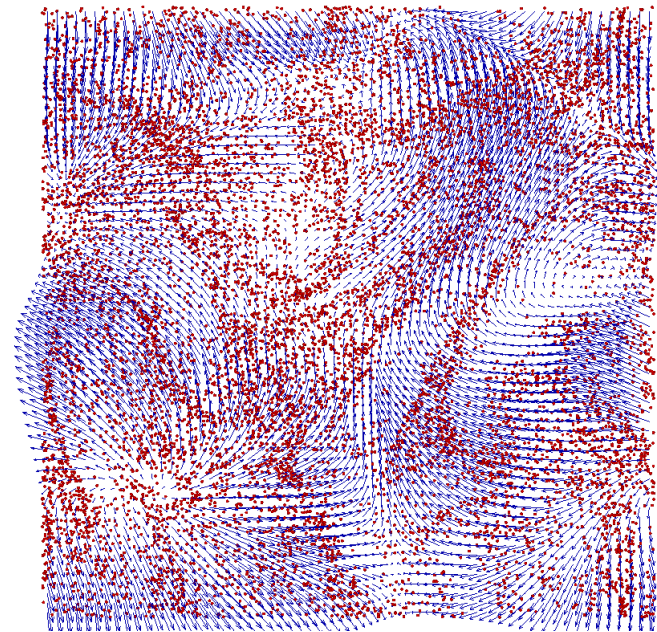
Introduction

Motivation

- Field of application:
 - use DNS results in pure Euler/Lagrange simulations or in the frame of a hybrid scheme (agglomerate formation in colloidal systems)
 - assumptions: low Stokes numbers, low particle concentration



Coupling E./L. and DNS in hybrid approach



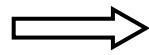
Lagrangian particles in isotropic turbulence

Numerical Method - LBM

Probability distribution function

- introduction of a density distribution function f :
 - instead of a deterministic modeling of molecular processes a reduced statistical approach is used to characterize the particle state
 - describes the probability of a fluid element to be at a certain time at a certain place having a certain momentum

$$f = f(\mathbf{x}, \boldsymbol{\xi}, t)$$



macroscopic properties are related to the moments of the probability function:

$$\rho = \int_{\xi_i=-\infty}^{\infty} f(\mathbf{x}, \boldsymbol{\xi}, t) d^3 \xi_i$$

$$\rho \mathbf{u} = \int_{\xi_i=-\infty}^{\infty} \boldsymbol{\xi} f(\mathbf{x}, \boldsymbol{\xi}, t) d^3 \xi_i$$

- Boltzmann equation:
 - describes the change of the distribution function and hence the fluid behavior

$$\frac{\partial f}{\partial t} + \boldsymbol{\xi} \frac{\partial f}{\partial \mathbf{x}} + \mathbf{F} \frac{\partial f}{\partial \boldsymbol{\xi}} = \Omega(f)$$

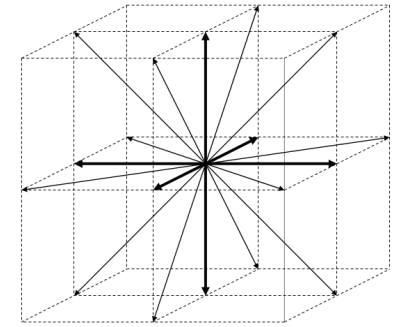
analytic solution (Maxwellian distribution) for special case:
ideal gas in thermodynamic equilibrium

Numerical Method - LBM

Lattice Boltzmann equation

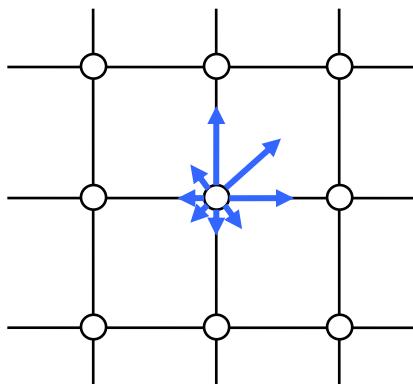
- Discretized BGK Boltzmann equation:
 - discretise space, time and velocity:

$$f_{\sigma i}(\mathbf{x} + \xi_{\sigma i} \Delta t, t + \Delta t) - f_{\sigma i}(\mathbf{x}, t) = -\frac{\Delta t}{\tau} (f_{\sigma i}(\mathbf{x}, t) - f_{\sigma i}^{(0)}(\mathbf{x}, t))$$

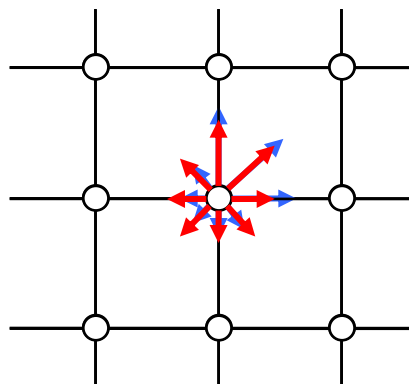


velocity directions of the D3Q19-Model

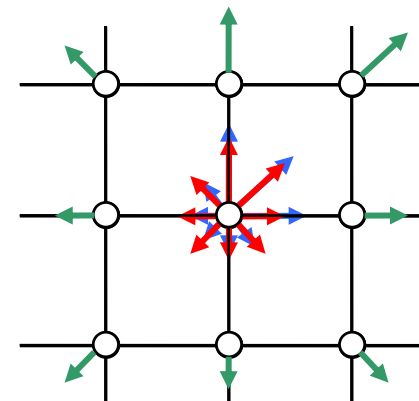
- iteration loop: relaxation & propagation:



Point of time: t



Point of time: t^+

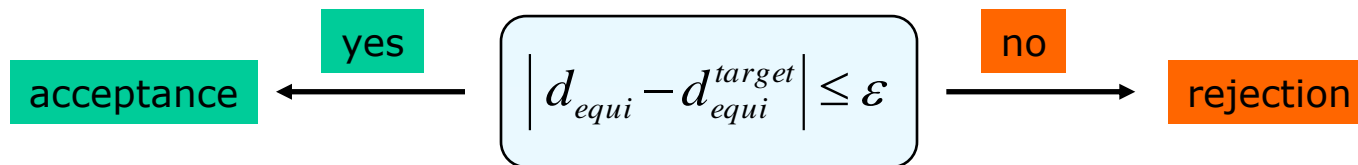
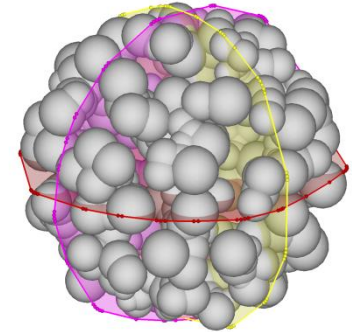


Point of time: $t + \Delta t$

Agglomerate model

Procedure of agglomerate generation

- Agglomerate generation based on random growth plus design specifications:
 - creation by definition of:
 - number and size distribution of primary particles
 - optional sintering of contact points
 - morphological type (*dendritic, spherical clusters, flocks*)
 - target quantity
 - determination of particle characteristics:
 - equivalent diameters (also as basis of Reynolds and fluid dynamic coefficients)
 - porosity (e.g. based on convex hull) as main structural parameter
 - rejection sampling:
acceptance or rejection of the created agglomerates based on target parameters



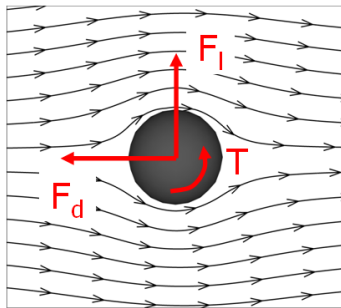
Agglomerate model

Definition of coefficients

- Definition of drag, lift and torque coefficient as function of adequate equivalent measures

$$d_{equi} = \{ d_{VES}; r_{gyr}; d_{intercept}; d_{por}; d_{AES}; \dots \}$$

$$Re = \frac{u d_{equi}}{\nu}$$



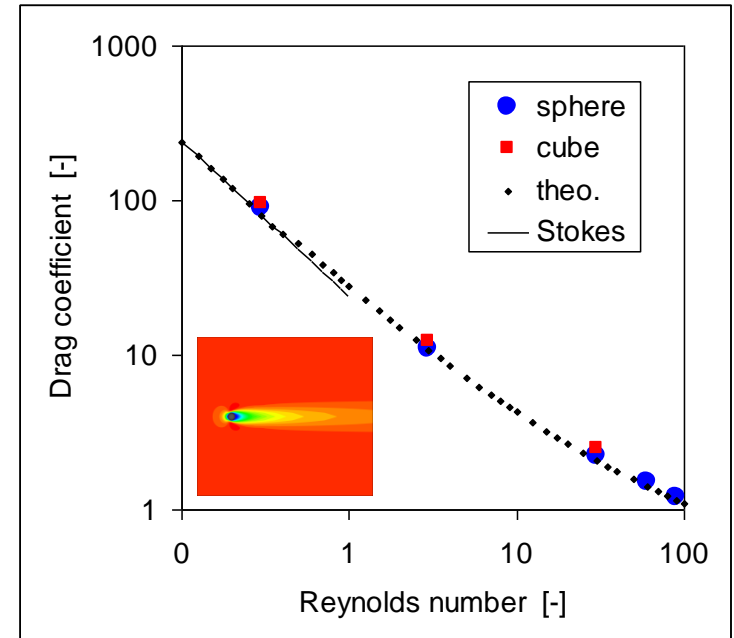
$$c_d = \frac{|\mathbf{F}_d|}{\frac{1}{2} \rho u^2 A_{equi}}$$

$$c_l = \frac{|\mathbf{F}_l|}{\frac{1}{2} \rho u^2 A_{equi}}$$

$$c_T = \frac{|\mathbf{T}|}{\frac{1}{2} \rho u^2 A_{equi} d_{equi}}$$

Validation

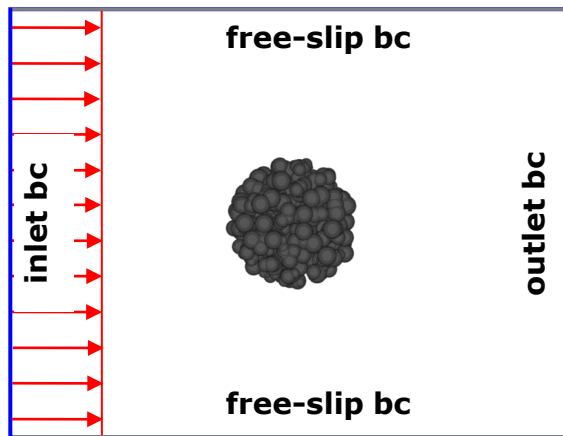
- Verification of forces and coefficients by simulating the flow around spheres and cubes (laminar flow regime)



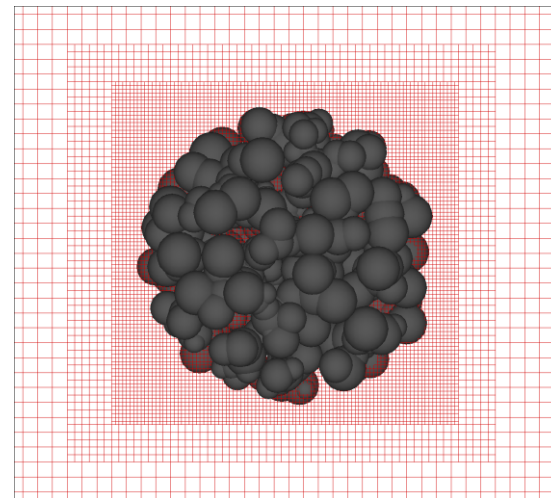
Parameter study

Numerical setup

- simulate 3d-flow around porous spherical agglomerates:
 - variation of morphology and mean porosity:
 - **group G1, G2:** clusters with porosity between 30 and 80 %
 - **group G3:** fractal flocks with porosity larger than 90 %
 - variation of particle Reynolds number and reference parameter
 - reference simulation with rigid sphere for wall effect correction



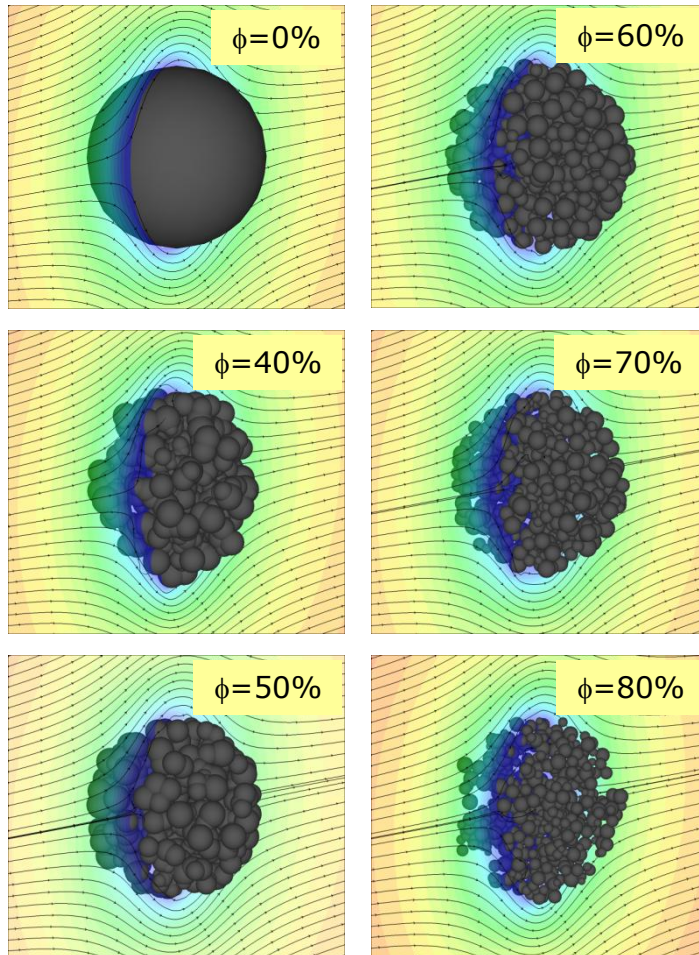
Schematic plot of numerical domain



Local grid refinement in the immediate vicinity of the agglomerate

Parameter study

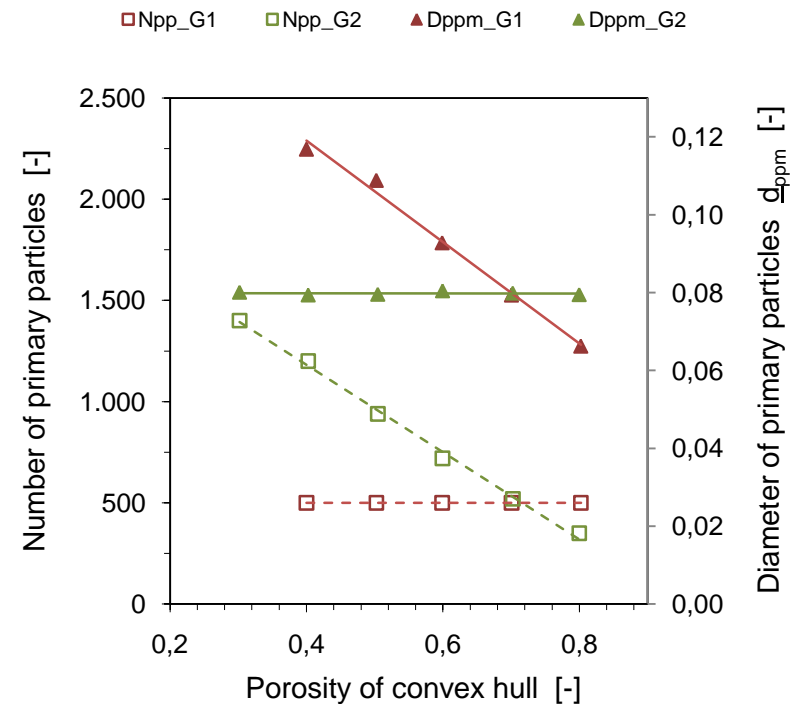
Clusters of group G1



Fluid field around particles at $Re=0.3$

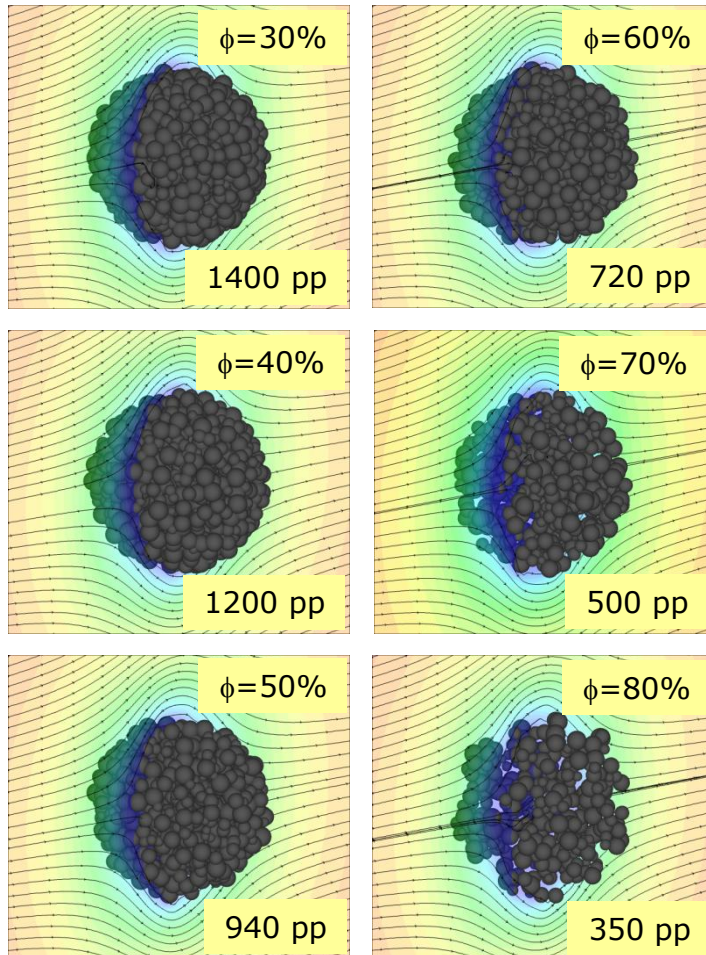
- particle size distribution, sintering at contacts
- **variation of mean primary particle size**
- **constant particle number: 500**
- variation of mean porosity: 40 ... 80 %

Structural parameters of G1 & G2



Parameter study

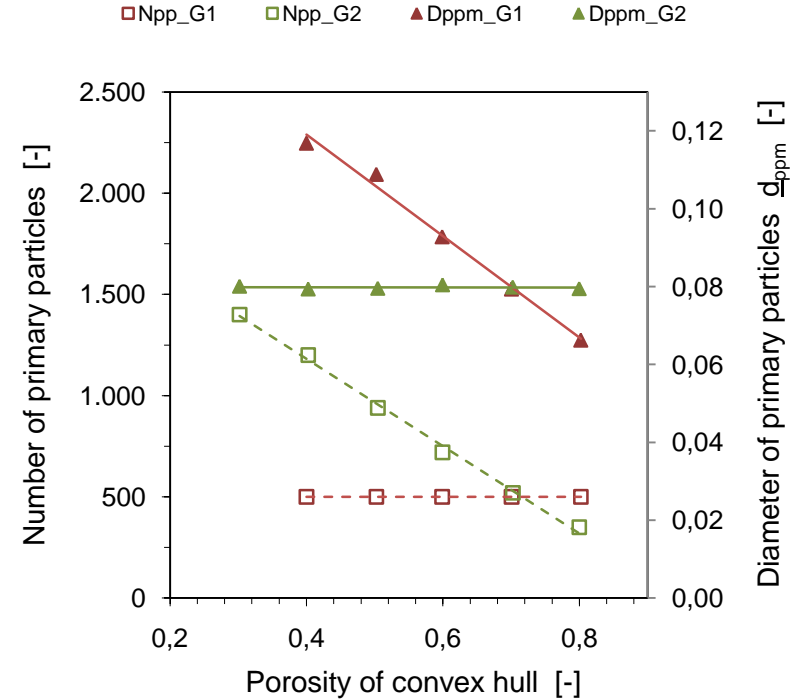
Clusters of group G2



Fluid field around particles at $Re=0.3$

- particle size distribution, sintering at contacts
- **constant mean primary particle size**
- **variation of particle number: 350 ... 1400**
- variation of mean porosity: 30 ... 80 %

Structural parameters of G1 & G2

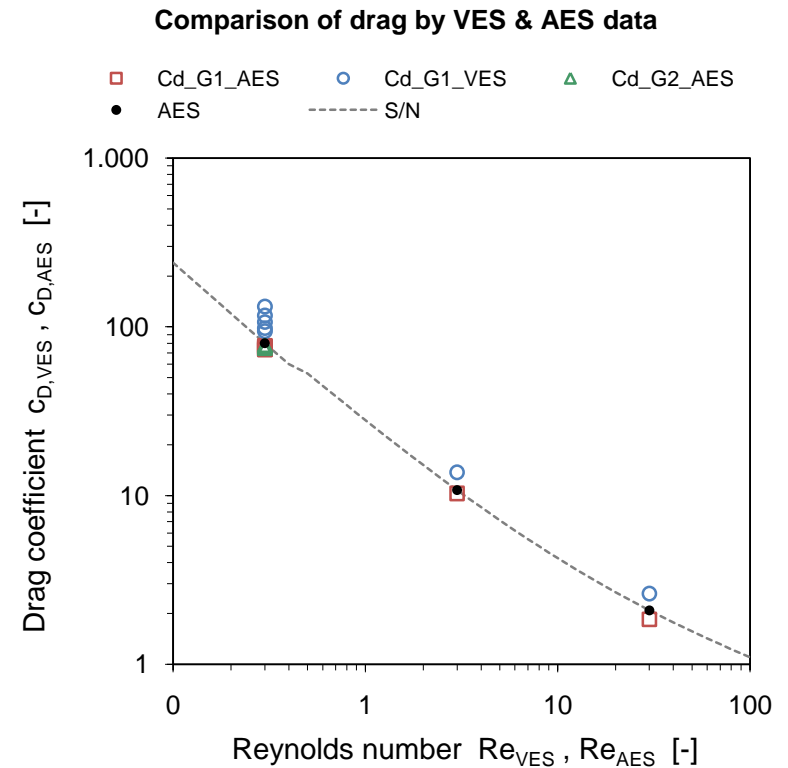
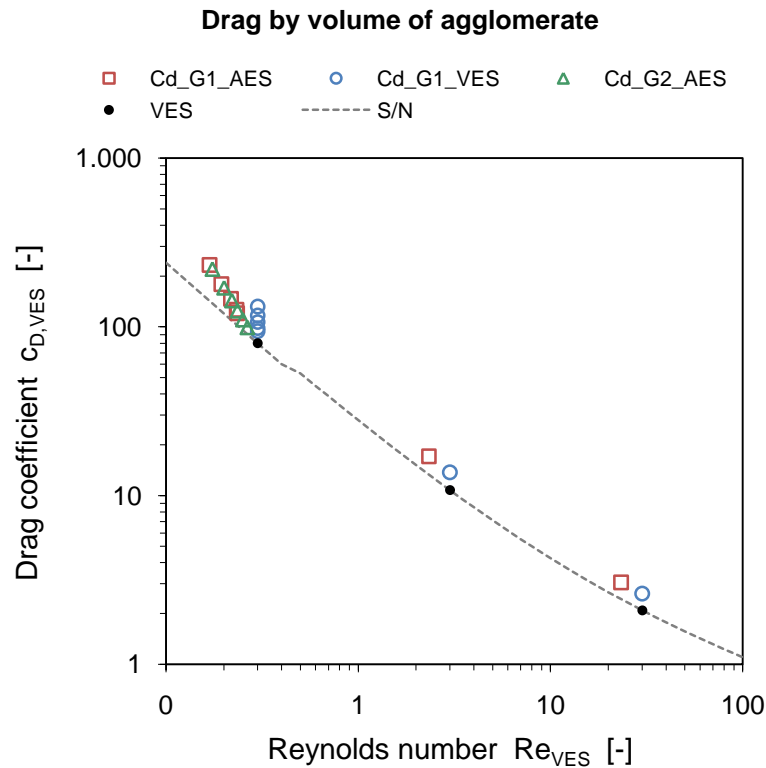


Parameter study

Drag coefficients of G1 & G2

Re = 0.3, 3.0, 30.0

- Influence of reference parameters for Re and drag:
 - G1 & G2 are generated with constant cross-sectional area of convex hull
 - simulation for constant area-based Re (G1, G2) and volume-based Re (G1 only)

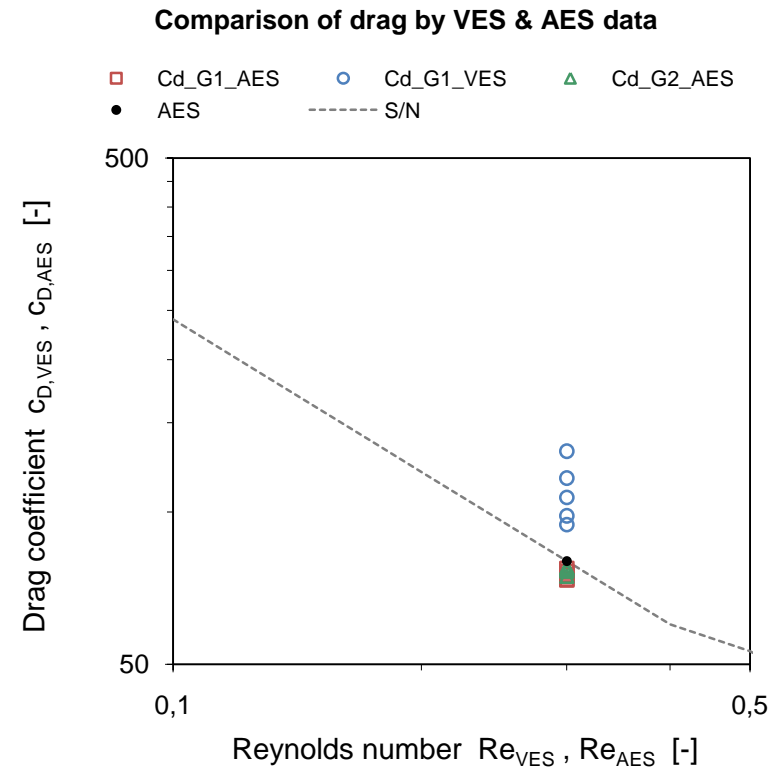
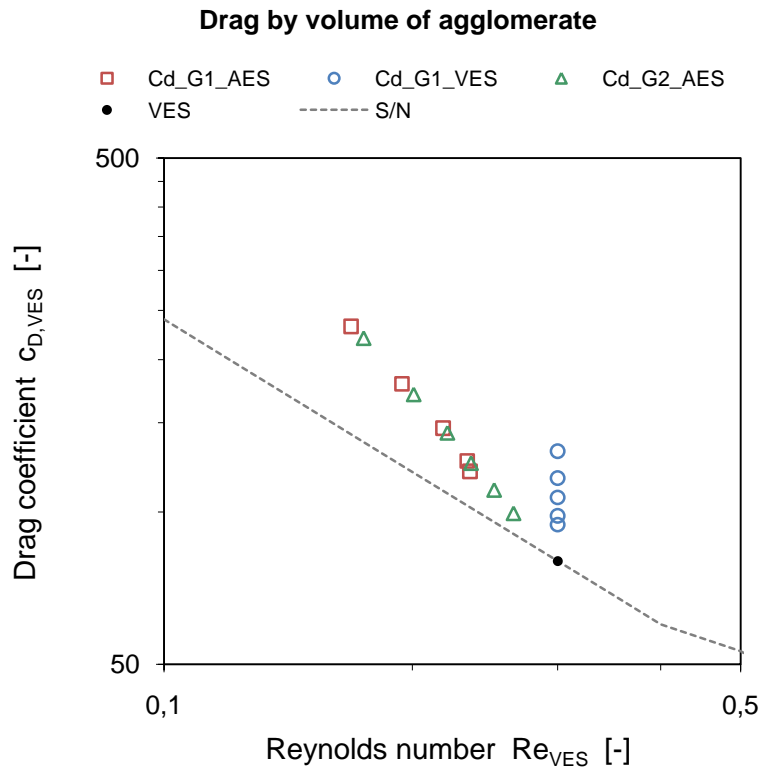


Parameter study

Drag coefficients of G1 & G2

Re = 0.3

- Influence of reference parameters for Re and drag:
 - VES-referred data documents an increase of drag
 - AES-based data is less spread and shows slight drag reduction



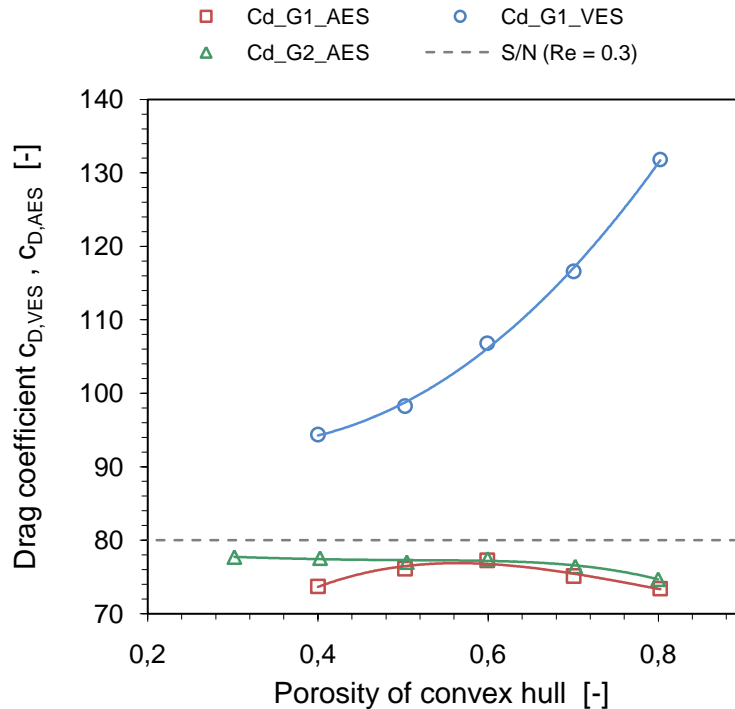
Parameter study

Drag coefficients of G1 & G2

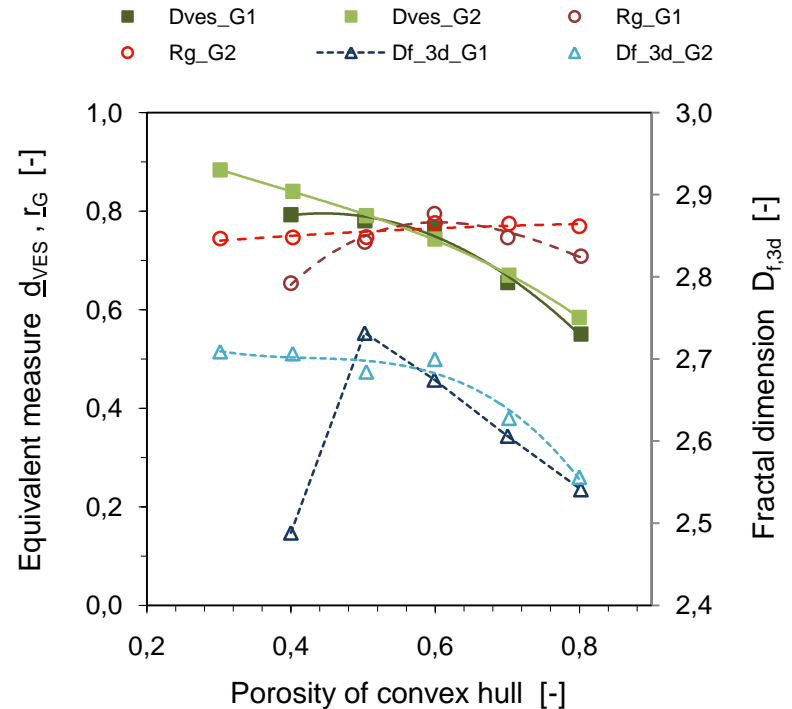
Re = 0.3

- Dependence of drag on agglomerate structure:
 - slight decrease of drag with increasing porosity (drop of 3–8 % compared to AES)
 - drop of drag for low porosity of G1 is related to structural differences (R_g , D_f)

Comparison of drag by VES & AES data



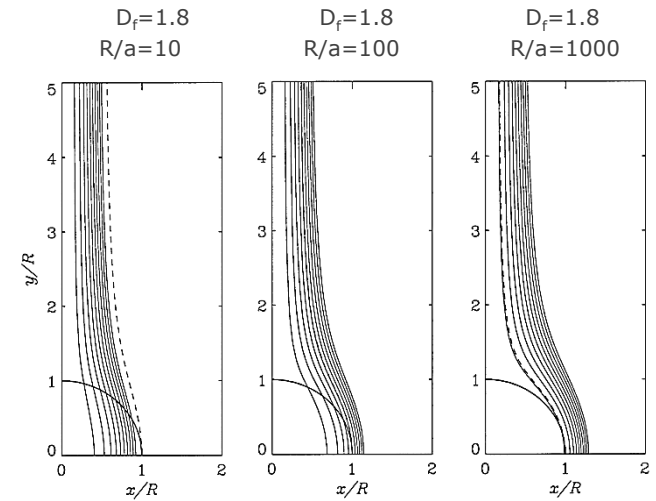
Particle properties of G1 & G2



Parameter study

Clusters of group G3

- Investigation of fractal agglomerates with different morphology:
 - basis: publication of Marco Vanni:
 - "Creeping flow over spherical permeable aggregates"
 - [Chemical Engineering Science 55, 2000, 685-698]
 - aggregates with fractal structure: radially varying solid fraction and permeability
 - assumptions: continuous porosity function, no local heterogeneities
 - Stokes equation for external flow and Brinkman equation for internal flow
 - Variation of diameter ratio R/a and fractal dimension D_f



Diameter ratio	Fractal dimension		Particle number	Solid fraction	Porosity	
R/a	D_f	D_f^*	N_{pp}	$1 - \phi$	ϕ	ϕ^*
50	1,5	1,5	145	0,001	0,999	0,999
50	1,8	1,8	611	0,005	0,995	0,995
50	2,1	2,2	2434	0,019	0,981	0,981
50	2,4	2,6	9356	0,075	0,925	0,930
10	1,8	1,8	34	0,034	0,966	0,971
100	1,8	1,8	2127	0,002	0,998	0,998

$$N_{pp} = C_s \left(\frac{R}{a}\right)^{D_f}$$

$$C_s = 0.414 D_s - 0.211$$

$$\bar{\varphi}(R) = C_s \left(\frac{R}{a}\right)^{D_f - 3}$$

Parameter study

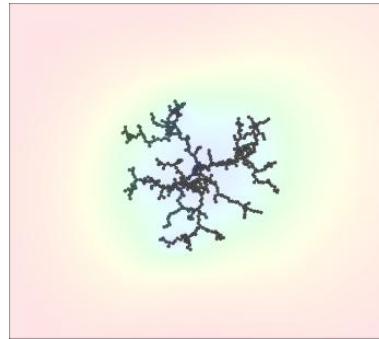
Clusters of group G3 with constant $D_f \approx 1.8$

- monodisperse, point contacts, constant primary particle size
- **variation of R/a : 10, 50, 100**
- **variation of particle number: 34 ... 2127**

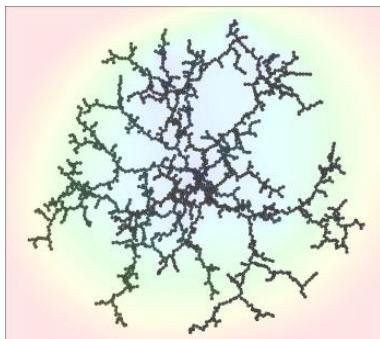
$R/a=10$



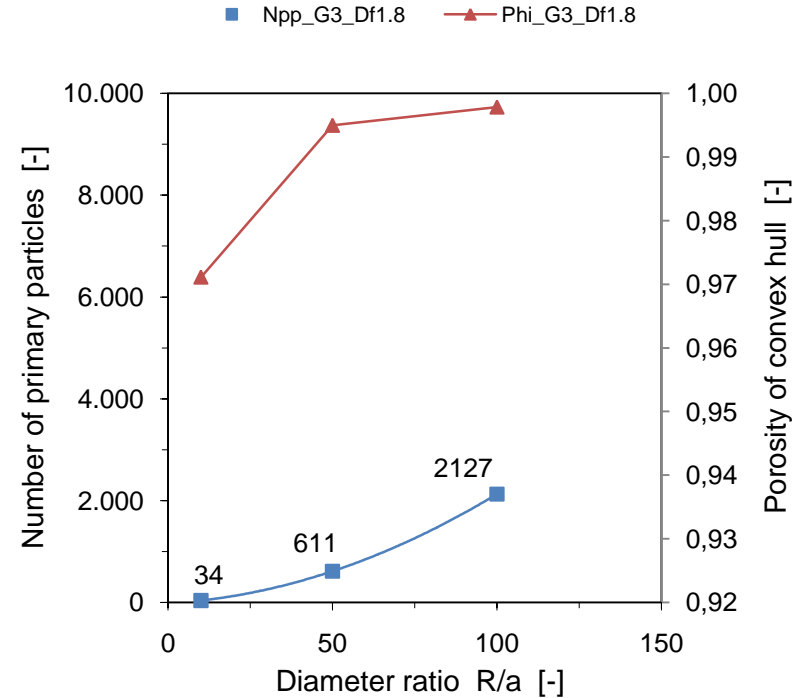
$R/a=50$



$R/a=100$



Structural parameters for $D_f \approx 1.8$

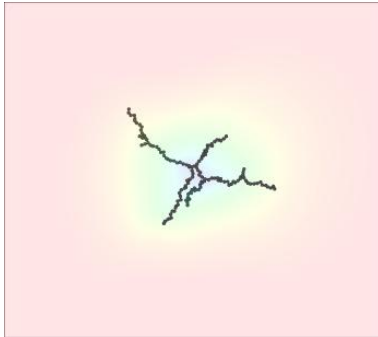


Parameter study

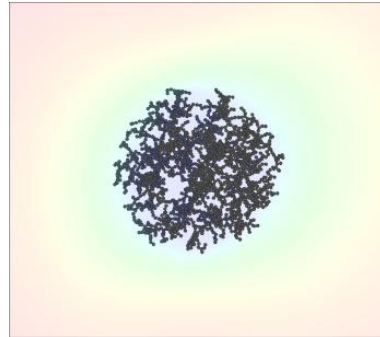
Clusters of group G3 with constant $R/a = 50$

- monodisperse, point contacts, constant primary particle size
- **variation of D_f : 1.5, 1.8, 2.2, 2.6**
- **variation of particle number: 145 ... 9356**

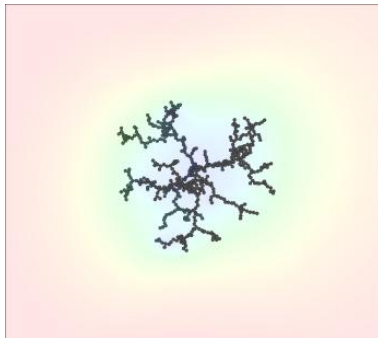
$D_f = 1.5$



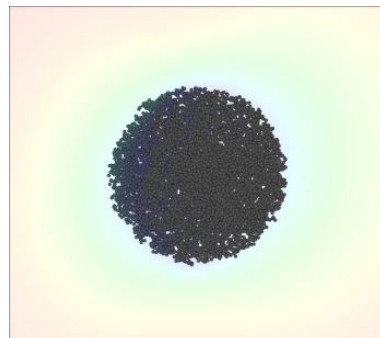
$D_f = 2.2$



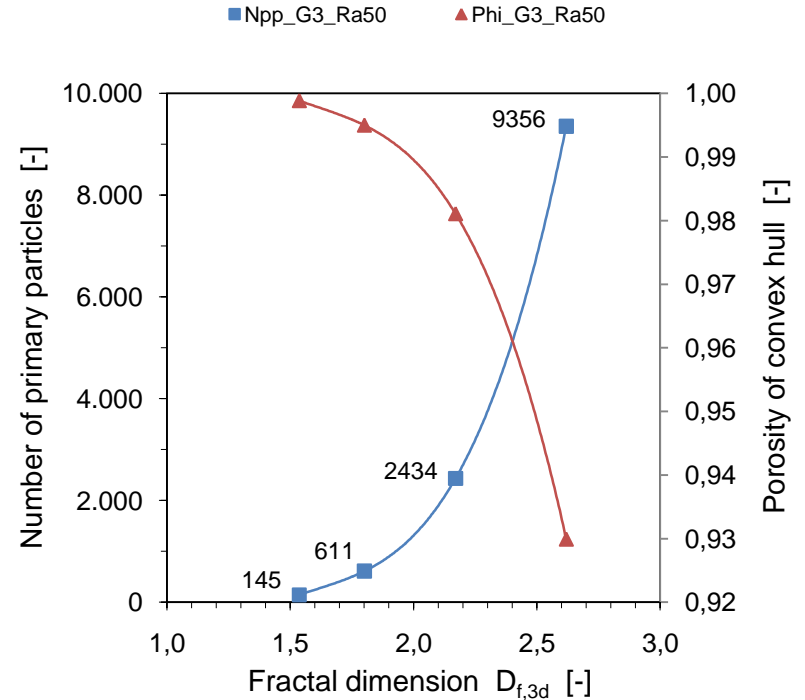
$D_f = 1.8$



$D_f = 2.6$



Structural parameters for $R/a = 50$



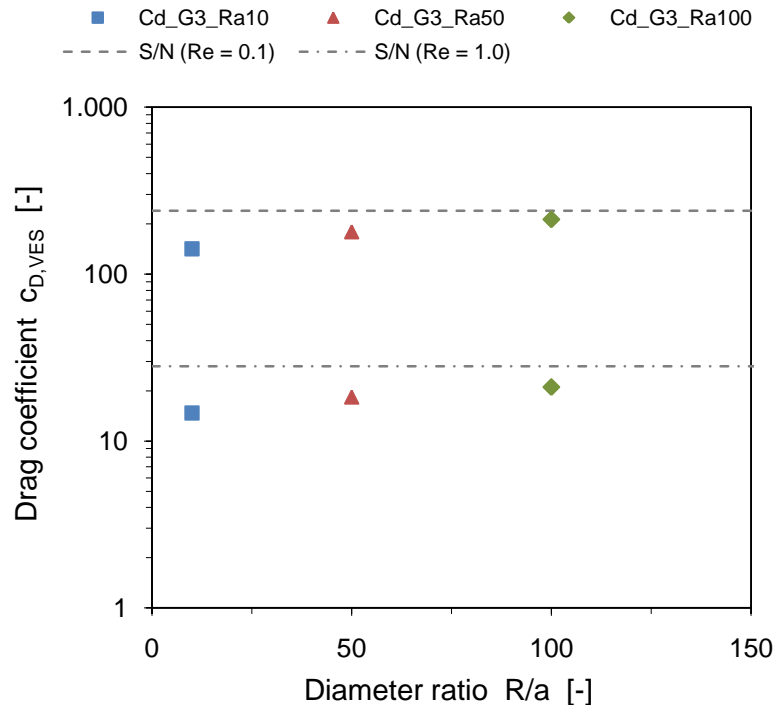
Parameter study

Drag of G3 with constant $D_f \approx 1.8$

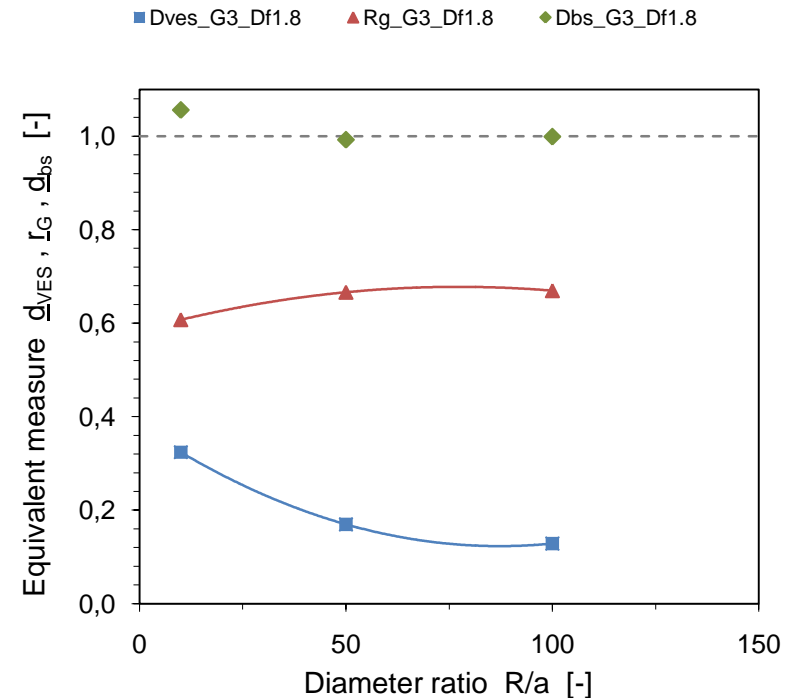
$Re = 0.1, 1.0$

- Influence of diameter ratio R/a :
 - Re and drag coefficient are referred to bounding sphere
 - drag reduction for low R/a (low particle number) in spite of lowest mean porosity

Drag by bounding sphere for $D_f \approx 1.8$



Particle properties for $D_f \approx 1.8$



Parameter study

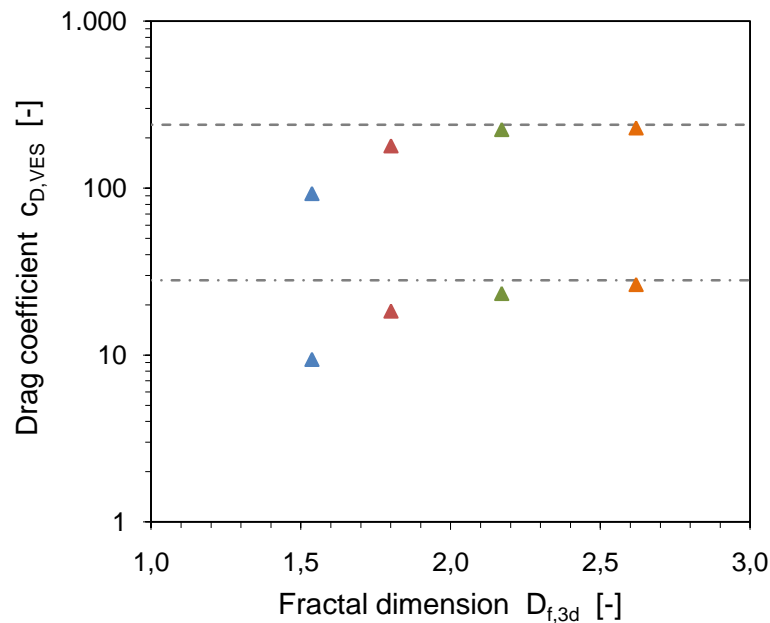
Drag of G3 with constant $R/a = 50$

$Re = 0.1, 1.0$

- Influence of fractal dimension D_f :
 - Re and drag coefficient are referred to bounding sphere
 - drag reduction for low D_f (low particle number) in accordance to highest mean porosity

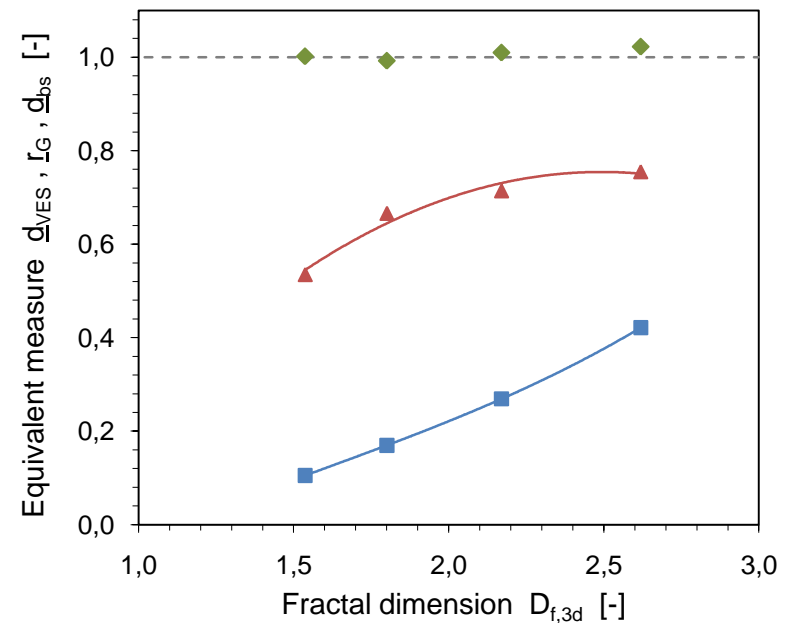
Drag by bounding sphere for $R/a = 50$

▲ $C_{d_G3_Df1.5}$ ▲ $C_{d_G3_Df1.8}$ ▲ $C_{d_G3_Df2.2}$
▲ $C_{d_G3_Df2.6}$ - - - S/N ($Re = 0.1$) - - - S/N ($Re = 1.0$)



Particle properties for $R/a = 50$

■ $D_{ves_G3_Ra50}$ ▲ $R_g_G3_Ra50$ ◆ $D_{bs_G3_Ra50}$



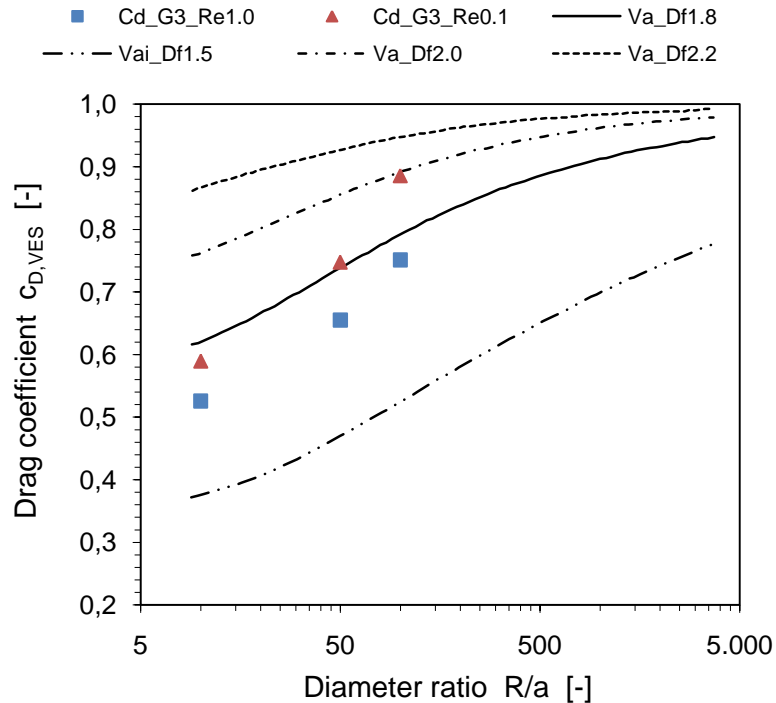
Parameter study

Drag reduction of G3

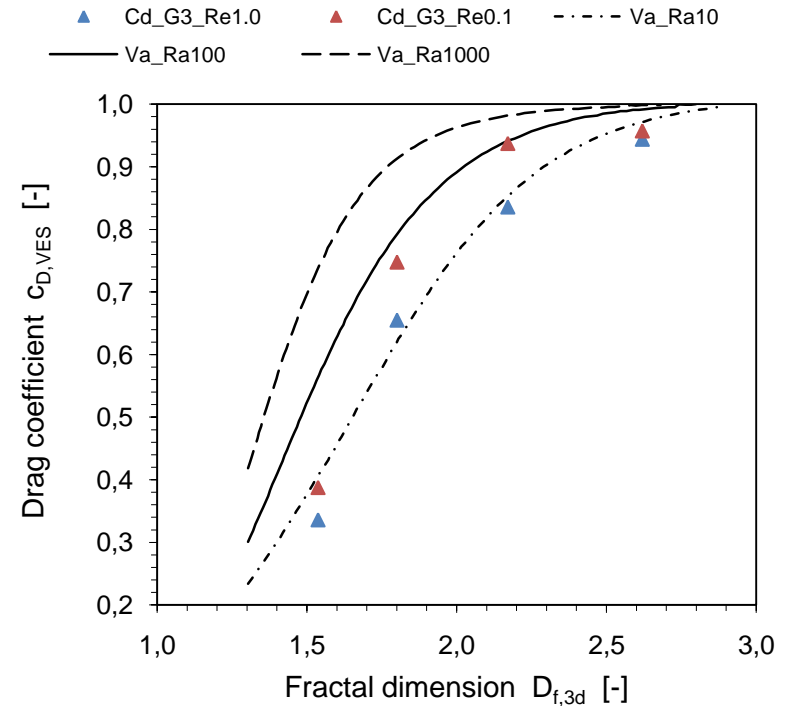
Re = 0.1, 1.0

- Comparison to the results of Vanni:
 - drag reduction seems to be more pronounced for Re=1.0 compared to 0.1
 - qualitative agreement with results of Vanni; differences may result from particle design or grid and domain size limitations

Drag reduction for $D_f \approx 1.8$



Drag reduction for $R/a = 50$



Conclusions

- investigation of the dependency of drag on particle morphology for different agglomerate types has been performed:
 - the hull-based cross-sectional area facing the flow or the bounding sphere diameter are useful as basis of the drag calculation of agglomerates
 - using the corresponding area- instead of the volume-equivalent diameter as reference parameter allows quantification of drag reduction
 - a moderate drag reduction was found for a wide range of agglomerate porosities in case of high fractal dimensions
 - a significant drop of the drag coefficient was found for porosities larger 90 % and a pronounced fractal structure of the agglomerates (porosity distribution)
 - LBM is capable to qualitatively reproduce drag reduction that is expected for fractal particles at Stokes flow regime

Acknowledgment



- The financial support of:
 - the German Federal Ministry of Education and Research (BMBF grant 03X3502D)
 - the Deutsche Forschungsgemeinschaft (DFG grant SO 204/36-1, SPP 1423)is gratefully acknowledged.

Collision integral

- Collision operator (multiple integral):
 - describes the contribution resulting from fluid element collision (collision number hypothesis)

- approximation by Bhatnagar-Gross-Krook (BGK):

$$\Omega(f) = -\frac{1}{\tau} (f - f^{(0)})$$

- BGK-Boltzmann equation:

$$\left(\frac{\partial}{\partial t} + \xi \cdot \nabla \right) f(\mathbf{x}, \xi, t) = -\frac{1}{\tau} (f(\mathbf{x}, \xi, t) - f^{(0)}(\mathbf{x}, \xi, t))$$

- equilibrium distribution f_0 :
(yields Maxwellian distribution for $\text{Kn} \ll 1$)

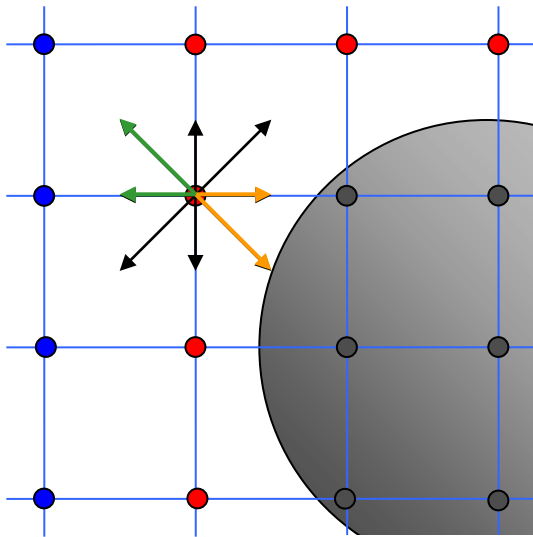
$$f^{(0)}(\mathbf{x}, \xi, t) = \frac{\rho}{(2\pi c_s^2)^{\frac{3}{2}}} e^{-\frac{(\xi - \mathbf{u})^2}{2c_s^2}}$$

- Chapman-Enskog analysis:
derivation of Navier-Stokes equations (including viscosity) from the Boltzmann equation in case of non-equilibrium states near the thermodynamic equilibrium

Numerical Method - LBM

No-slip boundary condition

- Calculation of forces at obstacles
 - momentum balance of the fluid along the obstacle surface
 - available for stepped and curved boundary condition
 - determination of the local forces at all fluid nodes near the obstacle
 - determination of the torque from local forces and there distance to the center of rotation (mass center)



Numerical grid near obstacle surface

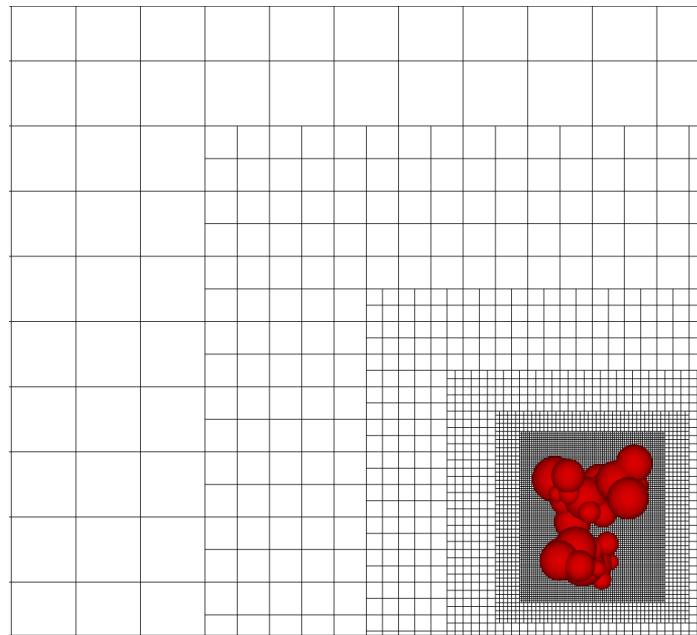
$$\mathbf{F}_{\sigma i}(\mathbf{x}, t + \Delta t/2) = \frac{\Delta V}{\Delta t} \left(f_{\sigma i}(\mathbf{x}, t + \Delta t) - f_{\sigma i}(\mathbf{x}, t^*) \right) \xi_{\sigma i}$$

$$\mathbf{T}_{\sigma i}(\mathbf{x}, t + \Delta t/2) = (\mathbf{x} - \mathbf{x}_R) \times \mathbf{F}_{\sigma i}(\mathbf{x}, t + \Delta t/2)$$

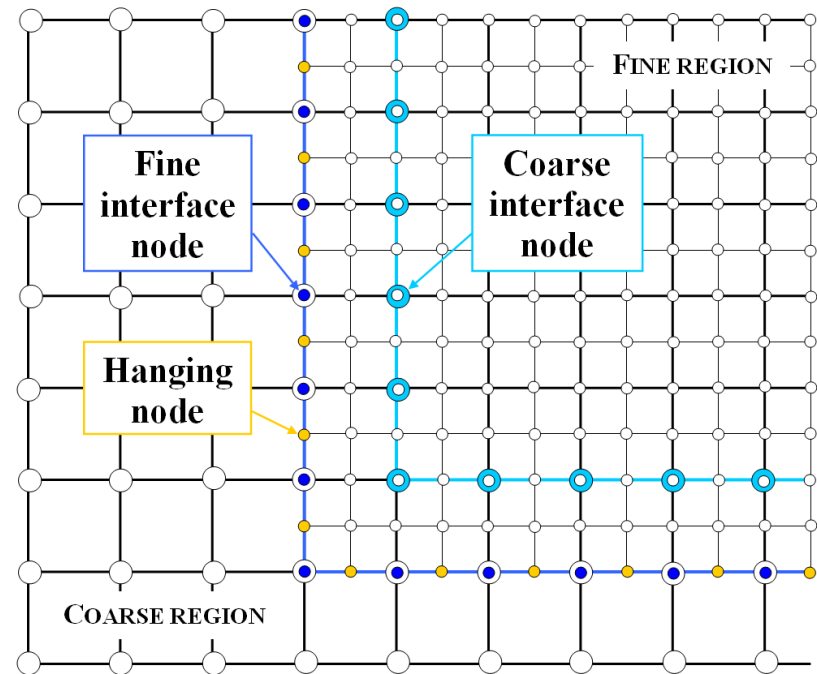
Numerical Method - LBM

Definition of local grid refinement

- local increase of the resolution of the numerical grid
 - increase accuracy of flow calculation, reduce numerical effort
 - data structure: cubic cells are represented by octal tree (B. Crouse)
 - coupling of grid regions with different resolution (exchange of information)



Stepwise grid refinement near agglomerate

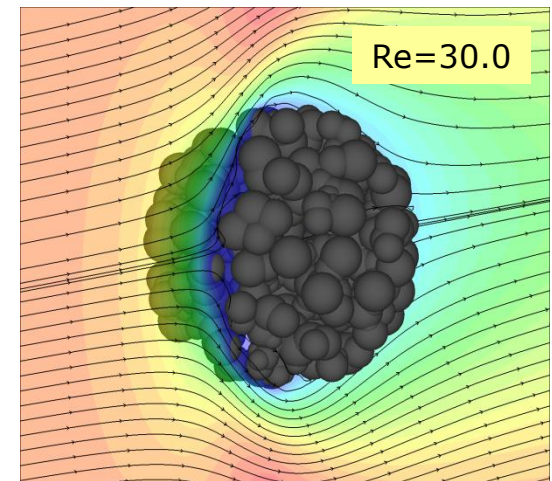
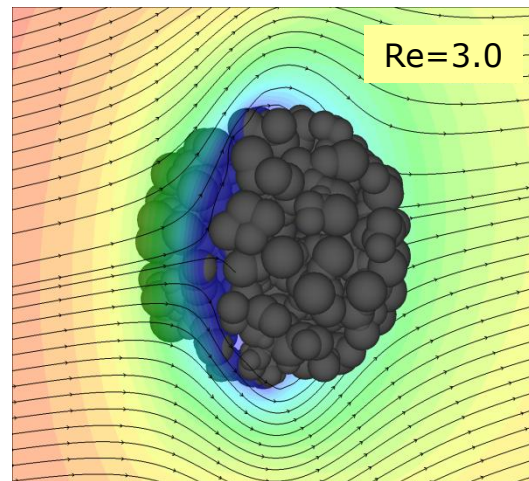
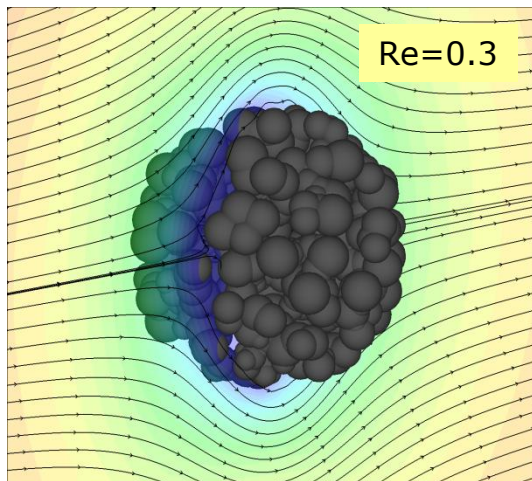


Nodal interface in-between fine & coarse grid region

Parameter study

Variation of fluid velocity

Set #1

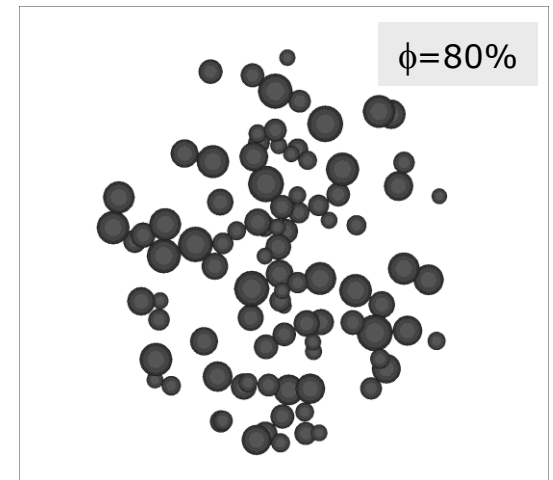
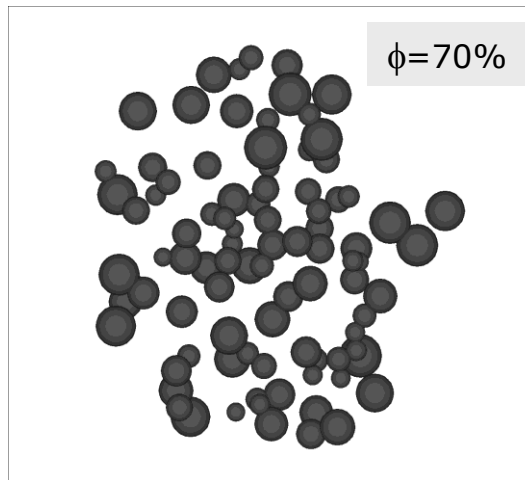
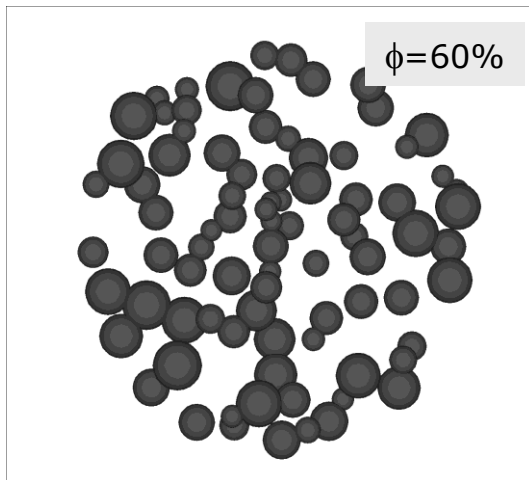
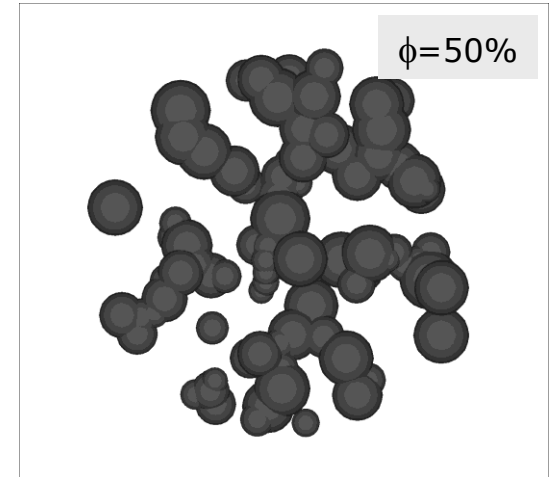
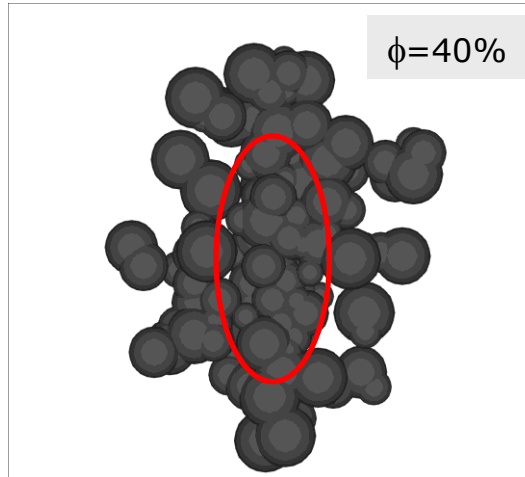
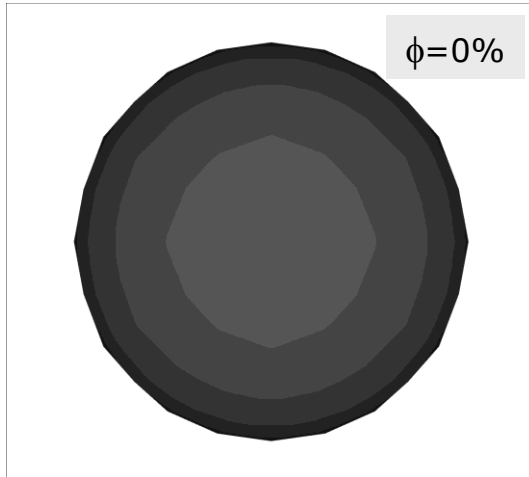


Comparison of fluid field around one agglomerate (*Set #1*, 500 p.p., porosity 50 %) at different Reynolds numbers

Parameter study

Primary particle distribution

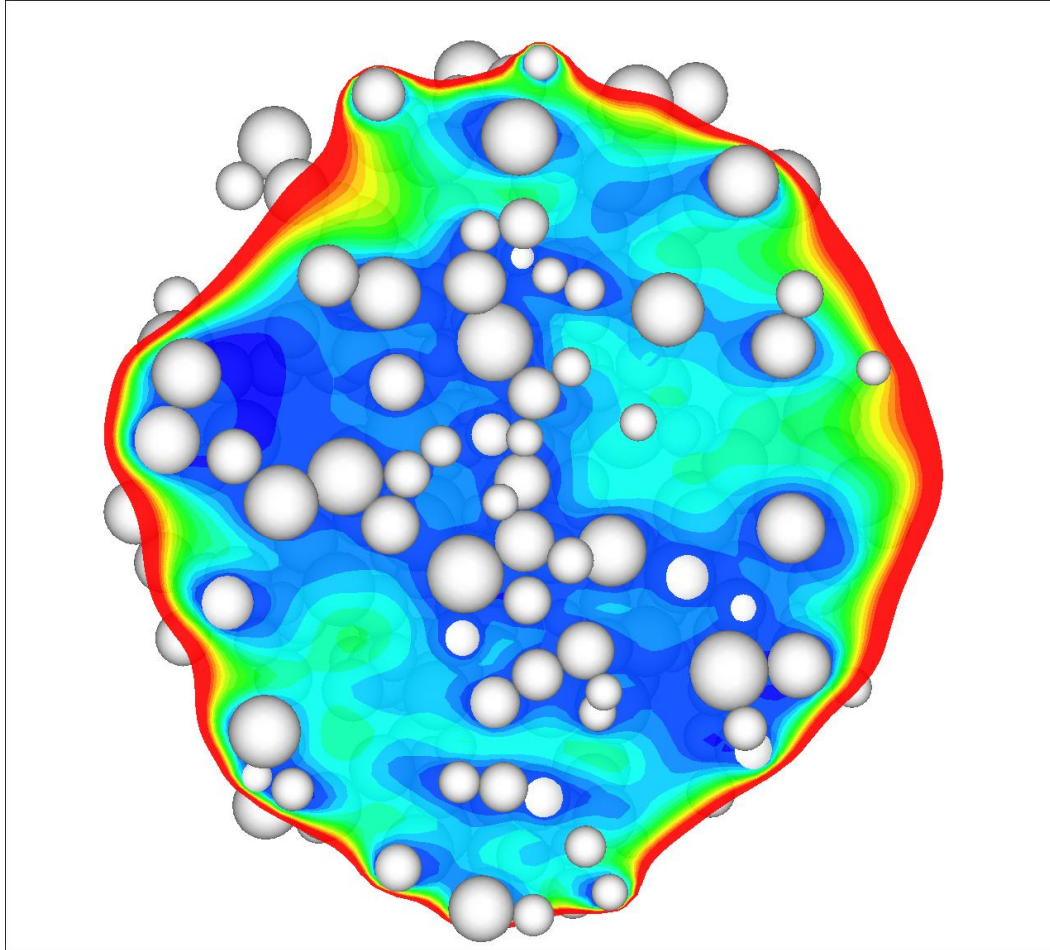
Set #1



Comparison of the particle distribution inside an identical center slice through the clusters

Permeability of the agglomerates

Set #1



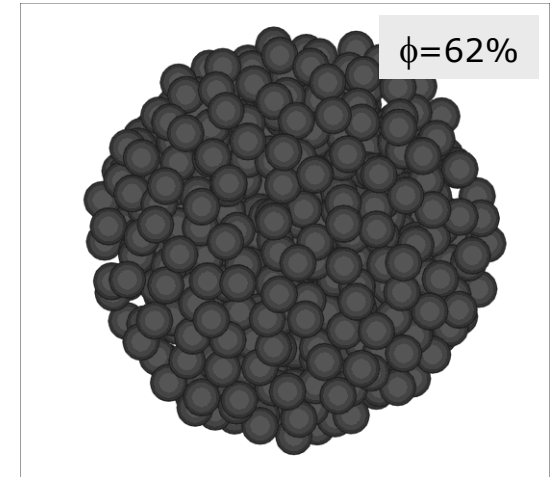
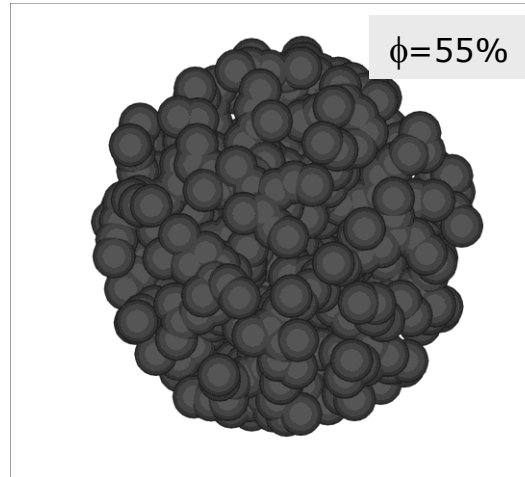
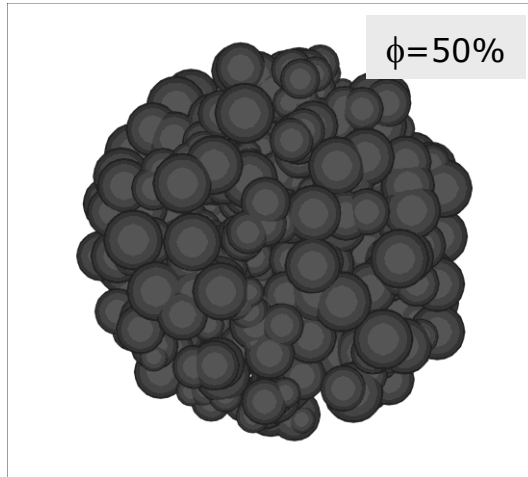
Mean velocity at the center cross section through the agglomerate

Sample:

- cluster with 500 p.p. & 80 % porosity
- about 5 grid cells per average primary particle diameter
- few stream traces are able to penetrate the agglomerate center
- the mean velocity inside the cluster is considerably below 1 % of the average fluid velocity ($Re = 0.3$)
- hence, a minor influence of the permeability on particle drag is expected for the present agglomerate model
- an uneven porosity distribution is likely to increase the impact on the drag force

Parameter study

Influence of particle size distribution and contact sintering on the box counting dimension



original setup:

500 pp.

polydisperse

contact point sintering

$\Phi = 50.2 \%$

$D_{f,bc,3d} = 2.73$

$D_{f,bc,2d} = 1.94$

monodisperse setup:

500 pp.

monodisperse

contact point sintering

$\Phi = 55.0 \%$

$D_{f,bc,3d} = 2.71$

$D_{f,bc,2d} = 1.94$

point contact setup:

500 pp.

monodisperse

point contacts

$\Phi = 62.2 \%$

$D_{f,bc,3d} = 2.68$

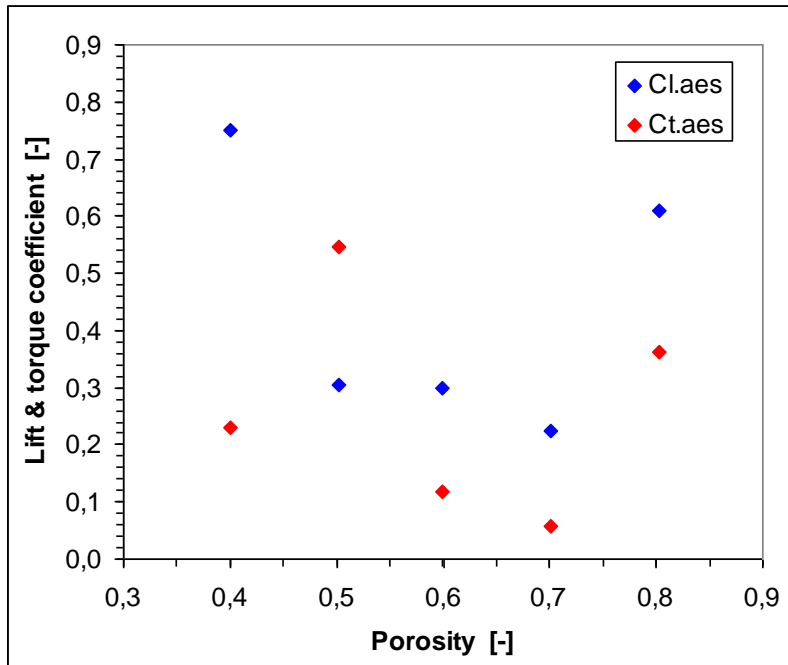
$D_{f,bc,2d} = 1.91$

Parameter study

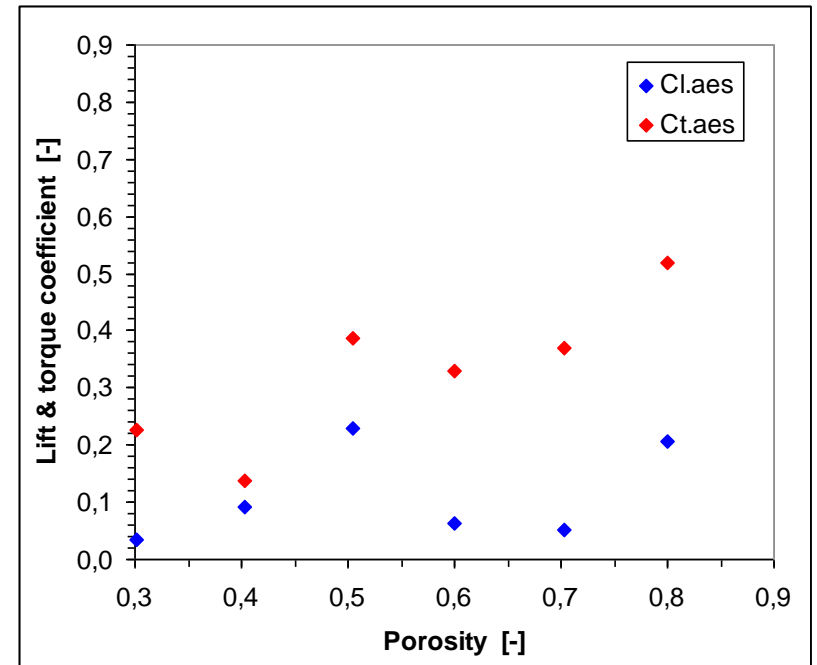
Lift & torque coefficient

Set #1, #2

- Reference parameter: cross-sectional area *in direction of flow*
 - no trend related to porosity (or fractal dimension) could be identified so far
 - correlation to the area perpendicular to the flow direction may lead to better results in case of the lift coefficient



Lift & torque of Set #1, Re = 0.3, por. 40...80 %



Lift & torque of Set #2, Re = 0.3, por. 30...80 %

Agglomerate model

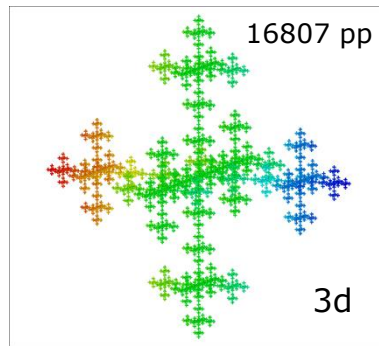
Agglomerate characterization – fractal dimension

- determination of fractal dimension by performing a box counting method

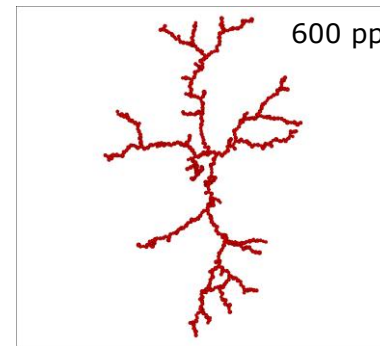
$$n_P = c \left(\frac{R}{r_P} \right)^{D_{f,n}}$$

$$D_{f,bc} = \lim_{\varepsilon \rightarrow 0} \left(\frac{\log(n_b)}{\log(\varepsilon)} \right)$$

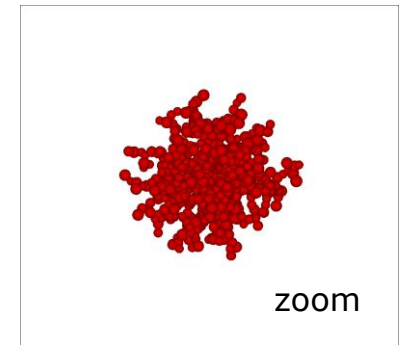
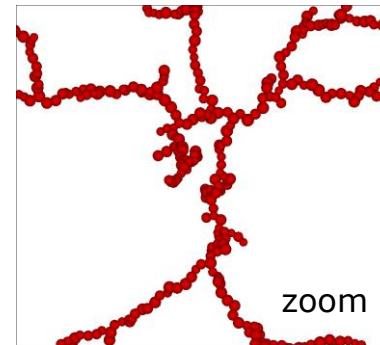
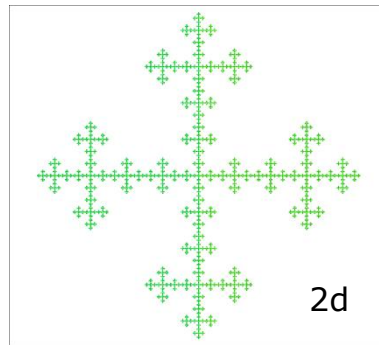
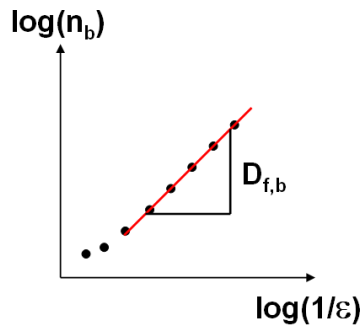
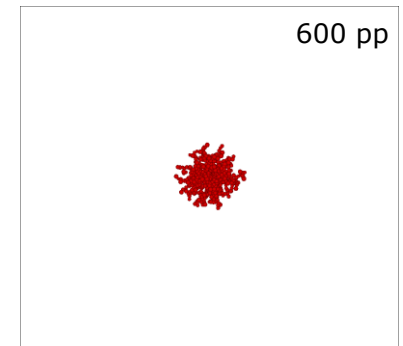
deterministic fractal



dendritic agglomerate



compact agglomerate



$D_{f,bc,3d}$: 1.79 ($\log 7 / \log 3 = 1.77$)

1.48

2.23

$D_{f,bc,2d}$: 1.50 ($\log 5 / \log 3 = 1.46$)

1.39

1.68